Effect of Annealing Temperature on Optical Transparency of Silica Xerogels

Majd M. Haddad, Muna S.A. Irnafeh*

Department of Physics, College of Science, University of Damascus, Damascus, SYRIA
* Corresponding author email: munirnafeh@gmail.com

Abstract
This letter explores the effect of annealing temperature in the range of 100-1000°C on the optical transparency of the xerogels synthesized by cryogenic compression technique. Results showed that the optical transparency of the synthesized xerogels showed a nonlinear behavior as it increased from <5% to 85% at 400°C and then sharply decreased to <15% at high temperatures (800-1000°C) due to the collapse of pores and formation of crystalline phases and defects within the structure.

Keywords: Xerogels; Thermal annealing; Optical transparency; Cryogenic compression technique
Received: March 2025; **Revised:** May 2026; **Accepted:** June 2026; **Published:** July 2026

1. Introduction

Xerogel materials have some unique physical properties that determine their uses and applications. Xerogels have porous structure with micropores (<2nm diameter) and mesopores (2-50nm diameter) [1]. The porosity and pore size reasonably depend on the preparation method, type of precursors, and drying conditions [2]. The distribution of pore size can be controlled by modifying the pH level, fractional amounts of reactants, and aging duration [3]. The surface area of xerogel is ranging in 100-1000 m^2/g. Such large surface area makes xerogel an ideal material for the applications requiring surface adsorption such as chemical catalysis and pollutant adsorption [4]. The density of xerogel is approximately ranging in 0.4-1.5 g/cm^3, which is higher than the density of aerogel (0.003-0.5 g/cm^3) but lower than that of conventional solid materials [5]. The density depends on shrinking degree during drying that can be reduced by enhancing the preparation conditions. Some types of xerogel show good transmissivity to the liquids and gases, which allows their use in filtering and separation applications [6].

The chemical properties of the xerogels are changing according to their chemical structures. The xerogel surface can be modified to be hydrophilic or hydrophobic by selecting the suitable precursors or performing post-production surface treatment [7]. Usually, functional groups such as hydroxyl (OH^-), carboxyl ($COOH^-$), or amine (NH_2^-) are exist on the xerogel surface as these groups determine the chemical reactivity and adsorption capability [8]. The xerogel mostly shows good chemical stability at the moderate conditions. However, it may be affected by the intensive acidic or basic conditions according to the material's type [9]. Silica xerogel – for instance – is stable in the neutral medium or slightly acidic but it dissolves in the basic medium [10]. Different functional groups can be introduced on or into the xerogel surface during preparation stage in sol-gel method or after the formation in order to enhance specific properties such as selective adsorption or catalytic activity [11].

The thermal properties of xerogel are very crucial for thermal insulation applications or high-temperature environments. Xerogels show relatively low thermal conductivity (0.03-0.2 W/m.K) due to the high content of air-filled pores, therefore, they are good thermal insulators [12]. Despite the thermal conductivity of xerogels is higher than that of aerogel (0.01-0.03 W/m.K), it still lower than that of the conventional materials like glass and concrete [13]. Thermal stability of the xerogel depends on its structure. Inorganic silica xerogel can hold temperatures up to 500-800°C before sintered and loosing porosity, while organic xerogel or hybrid (organic-inorganic) xerogel decomposes at lower temperatures (200-400°C) [14]. Thermal stability can be enhanced by incorporation of thermal stabilizers of consecutive heat treatments. Xerogels have medium specific heat capacities (0.5-1.5 J/g.K), which express their ability to store moderate amounts of heat [15]. Xerogels show relatively low thermal expansion coefficients that enhance their resistance to cracks or distortion when subjected to sudden thermal variations [16].

2. Experimental Part

The preparation process of xerogels includes several consecutive stages, each of them has crucial effect on the characteristics of the final product. In the

first stage, the foam solution was prepared by dissolving tetra ethyl ortho-silicate (TEOS) in water in presence of an acidic catalyst. The values of pH, temperature, and mixing fractions were optimized to achieve the required characteristics. After the sol was prepared, it was left to react and convert into wet gel throughout the polymerization and crosslinking reactions. During this stage, a 3D network was formed to trap the solvent inside its structure. The gel was aged for 12 hours to strengthen the network and increase the crosslinking level. The freezing stage is the most featured step in this technique as the wet gel was cooled down to -50°C at slow rate (5 °C/min) to allow the formation of relatively large ice crystals and hence large pores after removing the solvent. The gel was then directly immersed in liquid nitrogen to form ultrafine crystals. A pressure of $5x10^3$ Pa was applied on the sample to guide the growth of the crystals as well as to reduce the internal stresses. After completed freezing, the frozen gel was transferred to the lyophilizer to apply very low pressure (~0.5 mbar) while the temperature was gradually increased. Under these conditions, the frozen solvent directly converted into solid state and then sublimated to prevent the capillary forces from destroying the porous structure. Drying step can be carried out for 24 hours, but in this work, it lasted for 48 hours to guarantee the large shrinking leading to form xerogel. The prepared xerogel samples were subjected to heat treatment step at 400°C for 2 hours to enhance the chemical bonding and mechanical and thermal stability. In order to characterize the characteristics of the synthesized xerogel samples, the porosity, relative hardness and optical transparency were determined as functions of annealing temperature in the range of 100-1000°C with a step of 100°C. Figure (1) shows the synthesized xerogel samples.

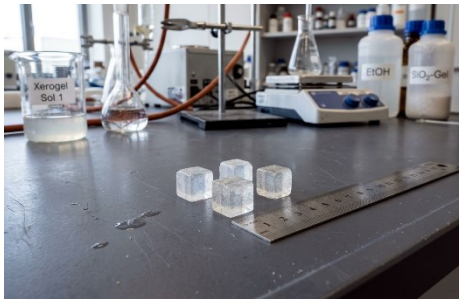

Fig. (1) Photograph of the synthesized Xerogel samples

3. Results and Discussion

Figure (2) shows the variation of the optical transparency of the synthesized xerogel samples with annealing temperature in the range of 100-1000°C. A complex and interesting behavior of transparency is observed as a function of annealing temperature. Different from the monotonic curves of porosity and relative hardness, the transparency shows non-monotonic behavior with initial increase, then gradual decrease upon exceeding an optimum temperature. This curve can be divided into three main regions. In the first region (<200°C), the transparency is very low (<5%) and linearly increases to reach ~45% at 300°C. This dramatic increase is attributed to several factors. At low annealing temperatures, the water and residual organic solvent evaporate as the presence of these liquids inside the pores causes light dispersion due to the difference in refractive indices between the liquid and surrounding solid material. When they are removed, the light dispersion is reduced and the transparency is enhanced. Also, some organic groups on the xerogel surface volatilize or decompose at temperatures of 150-200°C. This reduces the surface inhomogeneity and hence the light dispersion.

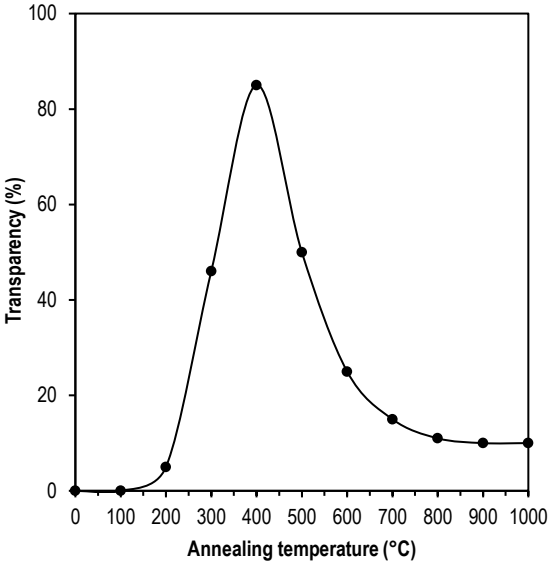

Fig. (4) Variation of the optical transparency of xerogel with annealing temperature

A slight and uniform shrink occurs in the porous structure, which increases the material strength and reduces light dispersion. It is important to notice that the transparency increases despite the relatively high porosity, which means that the existence of pores is not the only obstacle against transparency but their distribution, uniformity, and size with respect to the light wavelength (400-700nm) are important as well. The transparency reaches its maximum (~85%) at annealing temperature of 400°C then gradually decreases to 25% at 500°C. This is attributed to the removal of most solvent and surface organic groups while the pores still relatively small (<50nm) and the structure is homogeneous enough to reduce the light dispersion. Beyond 500°C, the transparency continues its decrease linearly to reach its minimum (<15%) at 800-1000°C as the material becomes completely opaque. This sharp decrease is a result of wide sintering and porous structure collapse, crystalline phase formation, increasing porosity, and

color change. The particles are merged and the small pores disappear, instead, very large pores form (larger than light wavelength) or structural defects cause strong dispersion of light. At temperatures exceeding 600-700°C, the material may start to convert from amorphous glassy phase into crystalline phases (such as cristobalite) and the crystalline grains act as strong centers for light dispersion. The overall porosity is reduced at high temperatures but the sizes of the remaining pores becomes relatively large (microscale) and these large pores cause highly-efficient light dispersion. At high temperatures, brown or grey color may appear due to the formation of color centers resulted from impurities or defects in the crystalline network, which increases light absorption.

4. Conclusion

In concluding remarks, the optical transparency showed a nonlinear behavior as its maximum of 85% was reached at 400°C and then sharply decreased beyond 500°C due to the collapse of pores and formation of crystalline phases. The optical characteristics of the synthesized xerogels can be controlled by selecting the appropriate annealing temperature for the desired application.

References

[1] D. Muringaniza et al., "Recent progress in synthesis and applications of monolithic metal–organic frameworks", *Mater. Adv.*, 7(1) (2025) 40-82.

[2] F. Baraka and J. Labidi, "The emergence of nanocellulose aerogels in CO_2 adsorption", *Sci. The Total Environ.*, 912 (2024) 169093.

[3] F.C. Lee et al., "Alternative architectures and materials for PEMFC gas diffusion layers: A review and outlook", *Renew. Sustain. Energy Rev.*, 166 (2022) 112640.

[4] G. Paterson et al., "Engine performance and emissions from a fumigated hydrogen/ammonia compression ignition engine with a hydrogen peroxide pilot", *Int. J. Hydro. Energy*, 67 (2024) 334-350.

[5] G.J. Owens et al., "Sol–gel based materials for biomedical applications", *Prog. Mater. Sci.*, 77 (2016) 1-79.

[6] J. Mu et al., "Phase-separated hydrogels for advanced biomedical engineering: From material design to applications", *Mater. Today Bio*, 38 (2026) 103096.

[7] J. Singh et al., "Tailoring carbon nanomaterial architectures for CO_2 capture: structure–property relationships, surface engineering, and future perspectives", *Mater. Adv.*, 7(6) (2026) 3031-3071.

[8] J.A. Santos et al., "Biopolymer-enhanced PVA hydrogels for DNA delivery: Structural and functional characterization", *Next Mater.*, 9 (2025).

[9] J.F. Conroy, M.E. Power and P.M. Norris, "Applications for Sol-Gel-Derived Materials in Medicine and Biology", *SLAS Technol.*, 5(1) (2000) 52-57.

[10] J.L. Plawsky, J.K. Kim and E.F. Schubert, "Engineered nanoporous and nanostructured films", *Mater. Today*, 12(6) (2009) 36-45.

[11] J.M. Kriegl, F.K. Forster and G.U. Nienhaus, "Charge Recombination and Protein Dynamics in Bacterial Photosynthetic Reaction Centers Entrapped in a Sol-Gel Matrix", *Biophys. J.*, 85(3) (2003) 1851-1870.

[12] J.-P. Boilot, T. Gacoin and S. Perruchas, "Synthesis and sol–gel assembly of nanophosphors", *Comptes Rendus Chimie*, 13(1–2) (2010) 186-198.

[13] K.-j. Chao, P.-h. Liu and K.-y. Huang, "Thin films of mesoporous silica: characterization and applications", *Comptes Rendus Chimie*, 8(3–4) (2005) 727-739.

[14] M. Ahamed et al., "Oxygen-vacancy engineering and junction design in CeO_2 nanomaterials for photocatalysis and antibacterial action: A review", *Result. Eng.*, 28 (2025) 108076.

[15] M.I.M. Kusdhany and S.M. Lyth, "New insights into hydrogen uptake on porous carbon materials via explainable machine learning", *Carbon*, 179 (2021) 190-201.

[16] MdS. Islam et al., "Carbon gel materials: synthesis, structural design, and emerging applications in energy and environmental technologies", *Mater. Adv.*, 6(20) (2025) 7153-7206.

